

ADVANCED MATERIALS

Supporting Information

for *Adv. Mater.*, DOI: 10.1002/adma.201804506

The Effects of Doping Density and Temperature on the
Optoelectronic Properties of Formamidinium Tin Triiodide
Thin Films

*Rebecca L. Milot, Matthew T. Klug, Christopher L. Davies,
Zhiping Wang, Hans Kraus, Henry J. Snaith, Michael B.
Johnston, and Laura M. Herz**

Copyright WILEY-VCH Verlag GmbH & Co. KGaA, 69469 Weinheim, Germany, 2018.

Supporting Information

The Effects of Doping Density and Temperature on the Optoelectronic Properties of Formamidinium Tin Triiodide Thin Films

*Rebecca L. Milot, Matthew T. Klug, Christopher L. Davies, Zhiping Wang, Hans Kraus, Henry J. Snaith, Michael B. Johnston, and Laura M. Herz**

Contents

1.	Additional Film Characterization	S2
	- Thickness determination	
	- SEM	
	- XRD	
2.	Drude Conductivity Model of GaAs and FASnI ₃	S4
3.	Charge-Carrier Dynamics	S5
	- Fits to photoconductivity transients	
	- Fluence-dependent OPTPS data	
	- Table of optoelectronic properties	
4.	Absorbance Spectra	S8
5.	Additional PL Characterization	S9
6.	Charge-Carrier Mobility	S11
	- Charge-carrier mobility calculation	
	- Sample-to-sample variation of mobility	
7.	THz Photoconductivity	S13
	- Fitting of photoconductivity spectrum at 5 K	
	- Additional photoconductivity spectra	
8.	References	S16

1. Additional Film Characterization

SnF ₂	Thickness (nm)				Mean	St. Dev
	Left Side	Center 1	Center 2	Right Side		
0%	350.7	354.9	357.3	341.4	351.1	7.0
5%	337.8	338.1	367.1	337.8	345.2	14.6
10%	336.9	326.3	357.1	335.4	338.9	13.0

Table S1. FASnI₃ film thicknesses determined from surface profilometry for samples to which different concentrations of SnF₂ had been added during fabrication. Measurements were performed using a Veeco Dektak 150 surface profilometer, and each sample was measured at four different points.

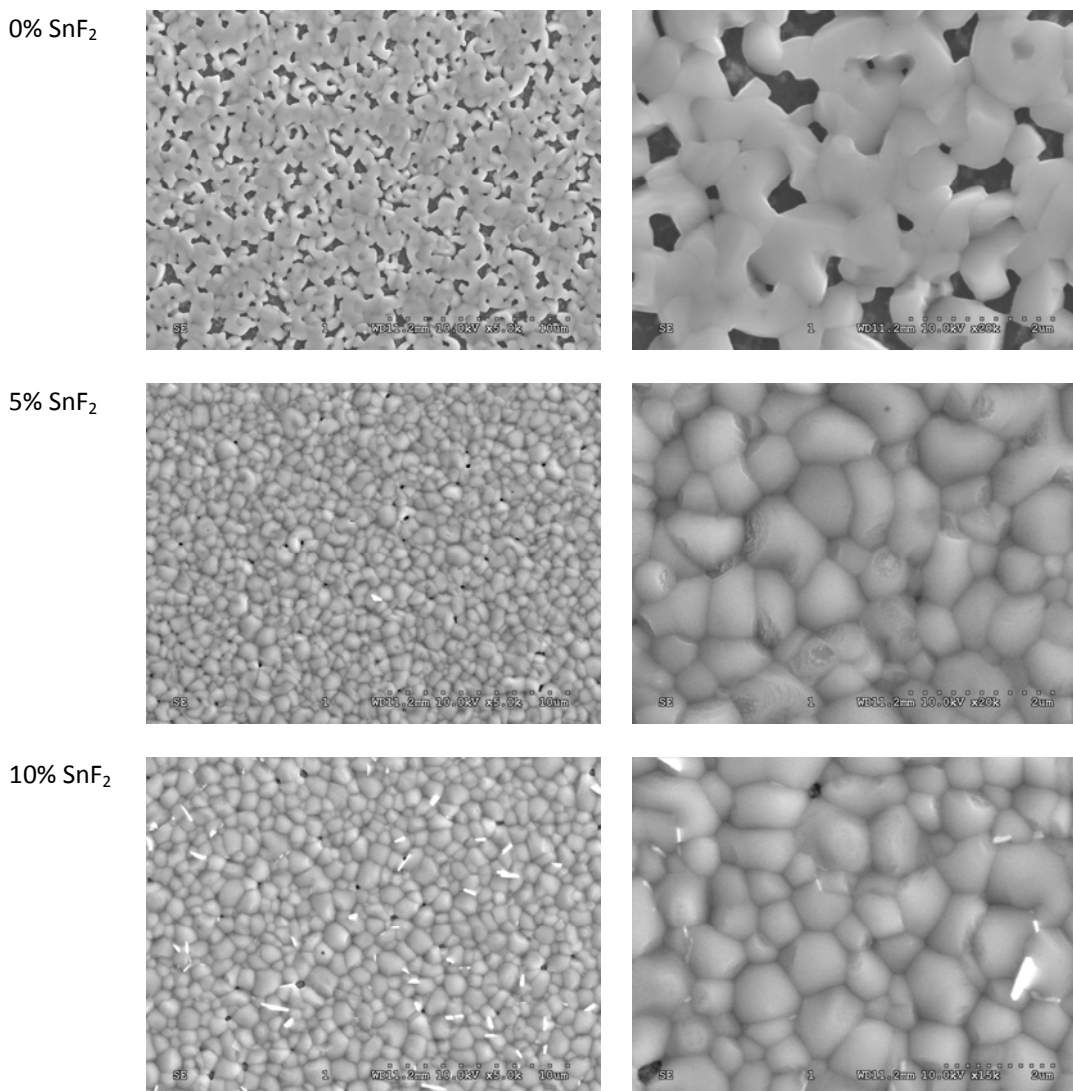


Figure S1. SEM micrographs of FASnI₃ thin films with various amount of SnF₂ molar excess prepared on FTO substrates. Imaging was performed using a Hitachi S-3400 SEM operating at 10 kV and 11 µA.

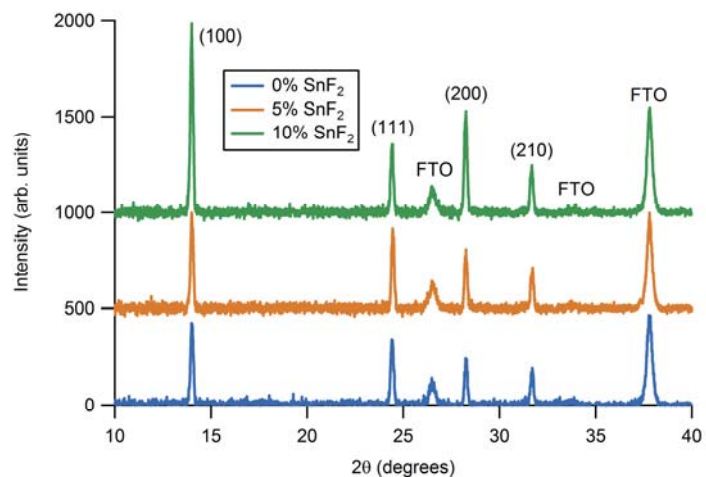


Figure S2. X-ray diffraction patterns for FASnI₃ films with 0%, 5%, and 10% added SnF₂ measured at room temperature. The traces for samples with 5% and 10% added SnF₂ have been offset from the baseline for clarity, and the peak labels apply to all three traces.

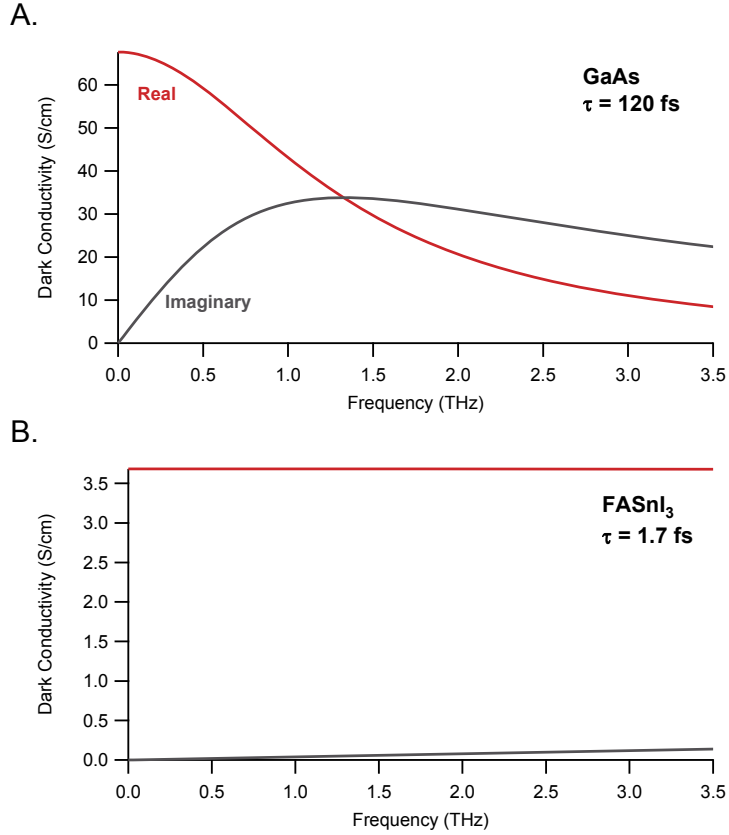
2. Drude Conductivity Model of GaAs and FASnI₃

Figure S3. Modelled real (red) and imaginary (gray) components of the Drude conductivity of GaAs (A) compared to FASnI₃ (B) at 295 K. For GaAs, the hole mobility is taken to be $420 \text{ cm}^2 \text{V}^{-1} \text{s}^{-1}$, and the heavy hole effective mass is $0.5m_e$, giving a scattering time of 120 fs.^[1] For FASnI₃, the scattering time is 1.7 fs, calculated from the estimated hole mobility value of the film with 10% added SnF₂ ($23.5 \text{ cm}^2 \text{V}^{-1} \text{s}^{-1}$, Table S2) and $m^* = 0.13m_e$, which is the hole effective mass estimated from GW calculations.^[2] A hole doping density of $N = 1 \times 10^{18} \text{ cm}^{-3}$ was used for both GaAs and FASnI₃. We used the expression $\sigma(\omega) = \sigma_0 (1 - i\omega\tau)^{-1}$ for the calculation of the conductivity, where the DC value is given by $\sigma_0 = p_0 e^2 \tau (m^*)^{-1} = p_0 e \mu$ where p_0 is the hole density, e the elementary charge, m^* the effective mass, τ the momentum scattering time, and μ the mobility of the charge carrier.

3. Charge-Carrier Dynamics

Fits to photoconductivity transients

As described in the main text, the overall recombination dynamics can be described by the following equation:

$$\frac{dn}{dt} = -k_2 n^2 - k_1 n, \quad (\text{S1})$$

where n is the photoexcited charge-carrier density, k_1 is the monomolecular rate constant, k_2 is the bimolecular rate constant. We neglect Auger processes, which we found to add only a minor relative component at the fluences investigated in this work.

As the experimentally observed quantity in optical pump-THz probe measurements, $\Delta T/T = x(t)$, is proportional to the photoconductivity, it is also proportional to the charge-carrier density.

$$n(t) = \varphi C x(t) \quad (\text{S2})$$

The photon-to-charge branching ratio φ indicates the fraction of absorbed photons which are converted to charge carriers. The proportionality factor $C = \tilde{n}_0/x(0)$ is the ratio of the absorbed photon density \tilde{n}_0 to the initial THz response at time zero $x(0)$, where

$$\tilde{n}_0 = \frac{E\lambda\alpha(\lambda)}{hcA_{\text{eff}}}(1 - R_{\text{pump}}). \quad (\text{S3})$$

The absorbed photon density is a function of the absorption coefficient α and reflectance R_{pump} of the sample at the excitation wavelength λ and of the effective overlap A_{eff} of the optical pump beam and THz probe beam. At high excitation fluences, $x(0)$ is no longer proportional to \tilde{n}_0 . The value of C is therefore determined using a value of $x(0)$ within the regime where $x(0)$ is linearly proportional to the excitation fluence.

An expression for the time-dependent THz dynamics can be obtained by substituting Equation S3 into Equation S1:

$$\begin{aligned} \frac{dx}{dt} &= -C\varphi k_2 x^2 - k_1 x \\ &= -A_2 x^2 - A_1 x \end{aligned} \quad (\text{S4})$$

with $A_i = C^{i-1}\varphi^{i-1}k_i$. The coefficients A_1 and A_2 , are determined via a global fit to a fluence dependent set of THz transients. As the photon-to-free-carrier conversion ratio φ is unknown, we can only determine the values φk_2 and k_1 from our fits. These equal the actual decay rate constants k_2 and k_1 in case the material exhibits full photon-to-free-charge conversion and are lower limits when $\varphi < 1$.

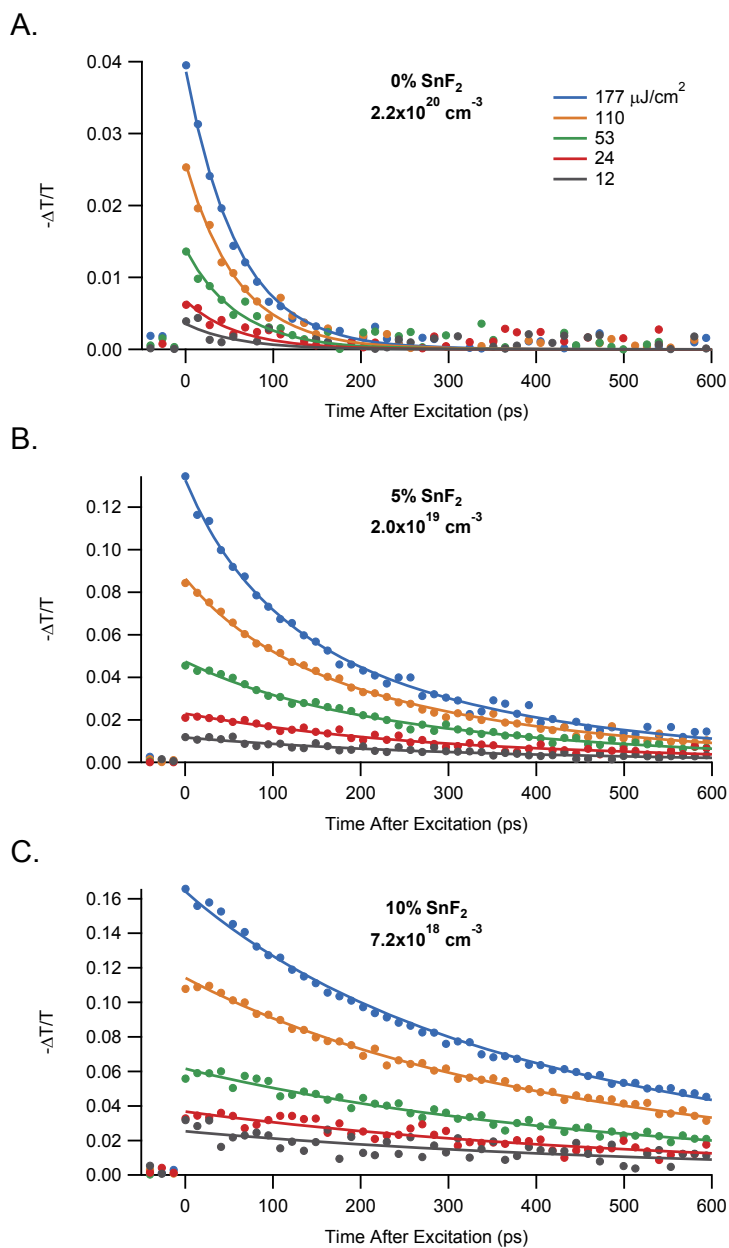


Figure S4. Fluence-dependent THz photoconductivity traces for FASnI₃ with added SnF₂ concentrations ranging from 0% to 10%. The samples were photoexcited at 800 nm at room temperature with fluences well below the amplified spontaneous emission (ASE) threshold as indicated in the figure legend. The experimental data were globally fit across all fluences according to Equation S4.

Table S2. Variation of the effective charge-carrier mobility μ , doping density p_0 , monomolecular recombination rate k_1 , effective bimolecular recombination rate constant k_2 , and charge-carrier diffusion length L_D at room temperature for FASnI₃ films with varying percentage of added SnF₂.

% SnF ₂	$\varphi\mu$ (cm ² V ⁻¹ s ⁻¹)	p_0 (cm ⁻³)	k_1 (s ⁻¹)	k_2 (cm ³ s ⁻¹)	L_D (nm)*
0	8	2.2x10 ²⁰	17x10 ⁹	-	35
5	29	2.0x10 ¹⁹	2.7x10 ⁹	2.3x10 ⁻¹⁰	165
10	47	7.2x10 ¹⁸	1.7x10 ⁹	0.7x10 ⁻¹⁰	265

*Calculated at a phototexcitation density of $n = 1 \times 10^{15}$ cm⁻³ using the expression

$L_D = \sqrt{D/R_{total}(n)}$. D is the diffusion coefficient with $D = \mu k_B T / e$, where μ is the charge-carrier mobility (taken to equal $\varphi\mu$ at room temperature, where excitons are dissociated), k_B is the Boltzmann constant, T is temperature (here 295 K), and e is the elementary charge. R_{total} is the total charge-carrier recombination rate given by $R_{total} = nk_2 + k_1$.

4. Absorbance Spectra

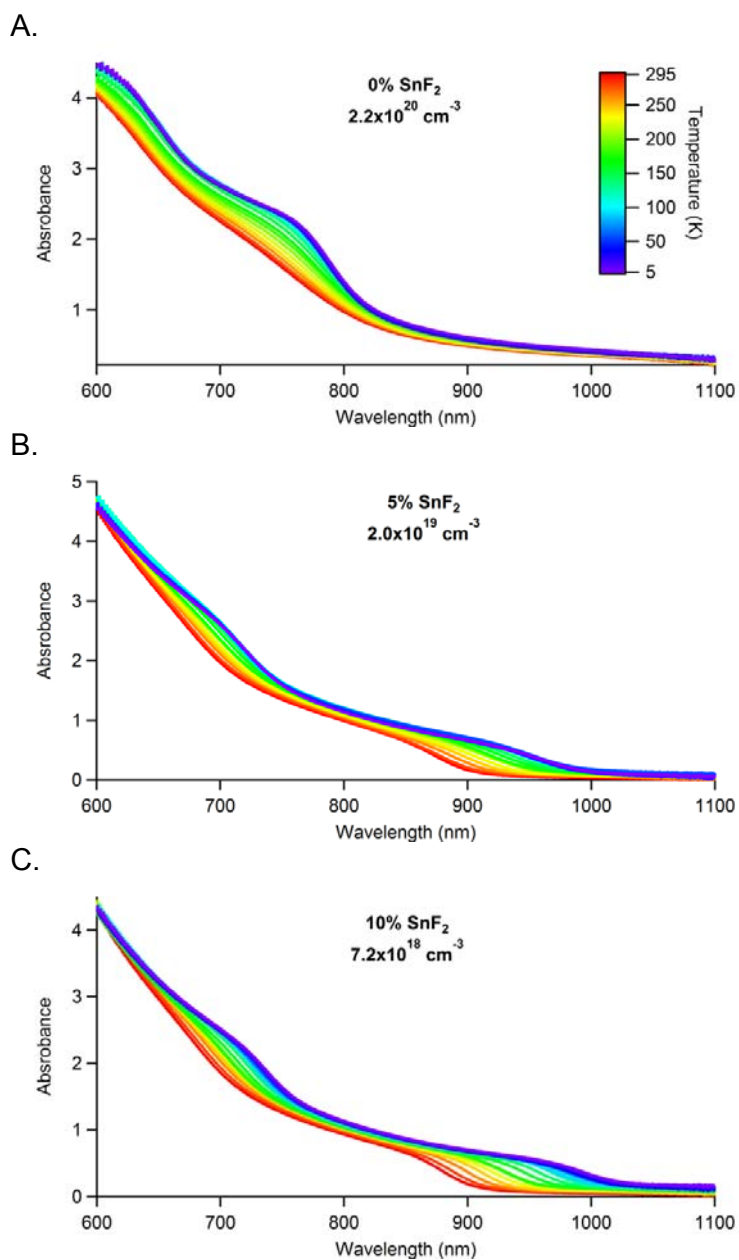


Figure S5. Absorbance spectra for films of FASnI₃ with (A) 0%, (B) 5%, and (C) 10% SnF₂ added during fabrication (top, middle, and bottom, respectively) recorded at temperatures ranging between 5 – 295 K.

5. Additional PL Characterization

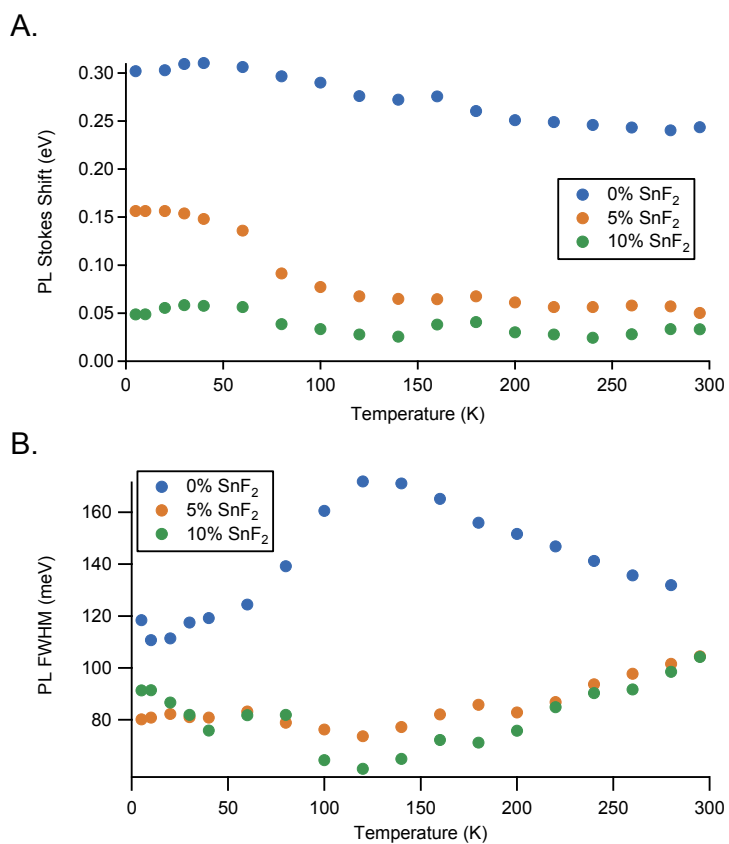


Figure S6. (A) PL Stokes shift calculated by the difference between the absorption onset midpoint (E_{abs}) and the PL maximum (E_{PL}). (B) Full width half maximum (FWHM) of the PL measured for films of FASnI₃ with 0%, 5%, and, 10% SnF₂ added during fabrication. All of the films were photoexcited at 800 nm with a fluence of 24 $\mu\text{J}/\text{cm}^2$.

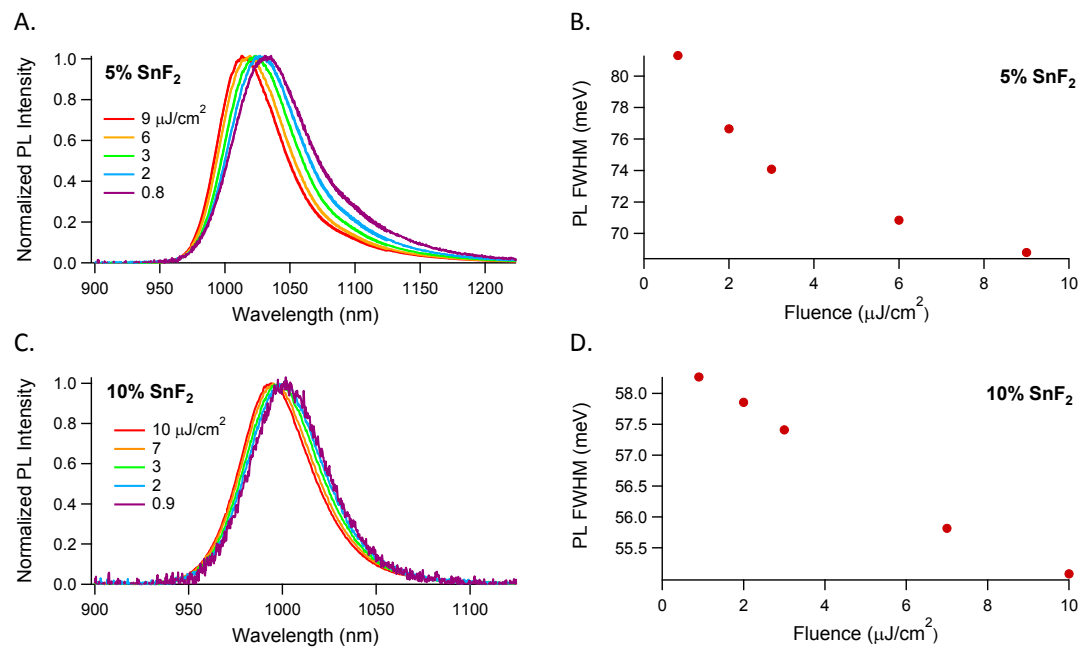


Figure S7. Normalized photoluminescence spectra for films of FASnI₃ with (A) 5% and (C) 10% SnF₂ added during fabrication measured at 5 K with photoexcitation at 800 nm with fluences ranging from 0.8 – 10 $\mu\text{J}/\text{cm}^2$. The relationship between FWHM of the PL peaks and the excitation fluence for films of FASnI₃ with (B) 5% and (D) 10% SnF₂ added.

6. Charge-Carrier Mobility

Charge-carrier mobility calculation

The charge carrier mobility μ is given by

$$\mu = \frac{\Delta S A_{\text{eff}}}{Ne}, \quad (\text{S5})$$

where ΔS is the sheet conductivity of the perovskite thin film, A_{eff} is the effective area of the overlap of optical pump and THz probe pulse, N is the number of photoexcited charge carriers, and e is the elementary charge.

Assuming that the film thickness is much smaller than the THz wavelength, the sheet photoconductivity ΔS of a thin film between two media of refractive indices, n_A and n_B , can be expressed as^[3-5]

$$\Delta S = -\varepsilon_0 c (n_A + n_B) \left(\frac{\Delta T}{T} \right), \quad (\text{S6})$$

where $\Delta T/T$ is the experimentally determined change in transmitted THz electric field amplitude. In our experiment, $n_A = 1$ for vacuum and $n_B = 2.13$ for the z-cut quartz substrate.

The number of photo-excited charge carriers N can be determined using the following equation:

$$N = \varphi \frac{E\lambda}{hc} (1 - R_{\text{pump}}) (1 - T_{\text{pump}}), \quad (\text{S7})$$

where E is the energy contained in an optical excitation pulse of wavelength λ , R_{pump} is the reflectivity of the sample at normal incidence of the excitation beam, T_{pump} transmittance of the pump beam, and φ is the ratio of free charge carriers created per photons absorbed (the photon-to-charge branching ratio).

Substituting Equations S7 and S6 into Equation S5, the following equation is obtained:

$$\varphi\mu = -\varepsilon_0 c (n_A + n_B) \frac{A_{\text{eff}} hc}{Ee\lambda (1 - R_{\text{pump}}) (1 - T_{\text{pump}})} \left(\frac{\Delta T}{T} \right). \quad (\text{S8})$$

Because $0 \leq \varphi \leq 1$, the effective mobility $\varphi\mu$ represents a lower limit, which becomes identical to the actual mobility for full photon to free carrier conversion. To allow accurate determination of $\varphi\mu$, we ensured that excitation conditions were in the linear regime. It should also be noted that the determined charge carrier mobility arises from the contributions of both electrons and holes and that these contributions cannot be separated.

As the laser frequency was near the band edge for the 0% sample (see Figure S8), a correction was performed to account for the changing absorption as a function of frequency. This correction was not needed for the FASnI₃ films with 5% and 10% added SnF₂, as their absorption spectra are red shifted compared to the 0% film.

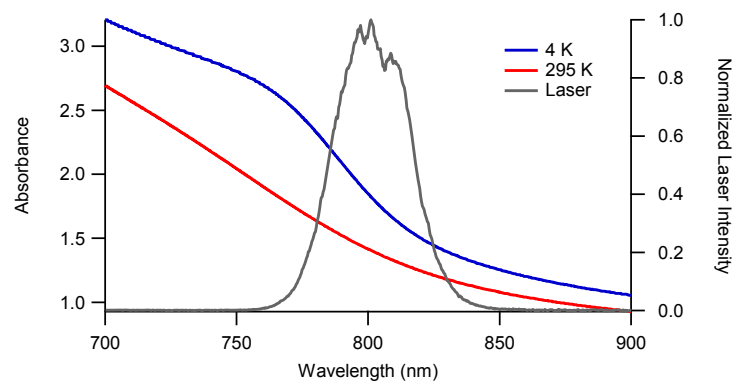


Figure S8. Absorbance of the FASnI₃ films with 0% added SnF₂ measured at 4 K and 295 K and compared to the 800-nm laser spectrum used for photo-excitation.

Table S3. Sample-to-sample variation of charge-carrier mobility at 295 K for FASnI₃ films with various percentages of SnF₂ added

Sample	Charge-Carrier Mobility (cm ² V ⁻¹ s ⁻¹)		
	0% SnF ₂	5% SnF ₂	10% SnF ₂
1	8	29	47
2	18	32	127
3	44	50	57
4			40
Average	23	37	68

7. THz Photoconductivity

Fitting of photoconductivity spectrum at 5 K

In semiconductors, excitonic states consist of discrete bound states and a continuum of unbound states analogous to a hydrogenic system. The photoconductivity response $\Delta\sigma$ is thus represented as a sum of the contributions for transitions from the 1s state to the np states and continuum states and is described as a function of the angular frequency ω by the sum of Lorentz oscillators with an oscillator strength given by Fermi's Golden Rule.^[5]

$$\Delta\sigma(\omega) \propto -i\omega\varepsilon_0 \left(\sum_{n=2}^{\infty} \frac{f_{1s \rightarrow np}}{\omega_n^2 - \omega^2 - i\omega\Gamma} + \int_{E_X/\hbar}^{\infty} \frac{f_{1s \rightarrow \infty}(\omega') d\omega'}{\omega'^2 - \omega^2 - i\omega\Gamma} \right), \quad (\text{S9})$$

where Γ is a broadening parameter, ε_0 is the permittivity of vacuum, ω_n is the transition energy, and $f_{1s \rightarrow np}$ and $f_{1s \rightarrow \infty}$ are the oscillator strengths for the $1s \rightarrow np$ and $1s \rightarrow \infty$ transitions, respectively.^[5] The exciton binding energy E_X is determined from

$$\omega_n = \frac{E_X}{\hbar} \left(1 - \frac{1}{n^2} \right) \quad (\text{S10})$$

As the contribution to the photoconductivity for transitions to the continuum states is negligible, we fit to the summation of the contributions from the $n = 1$ to $n = 40$ states only. To account for the presence of unbound charge-carriers, a Drude conductivity term was also included in the fit. As the scattering time for FASnI₃ is short, this term is estimated as a constant offset to the real part of the photoconductivity (see Section 2 above). The final fitting function is as follows:

$$\Delta\sigma(\omega) = -iA \sum_{n=2}^{40} \frac{\omega}{\omega_n^2 - \omega^2 - i\omega\Gamma} + C, \quad (\text{S11})$$

where A is a general proportionality constant and C is the real-valued constant Drude term.

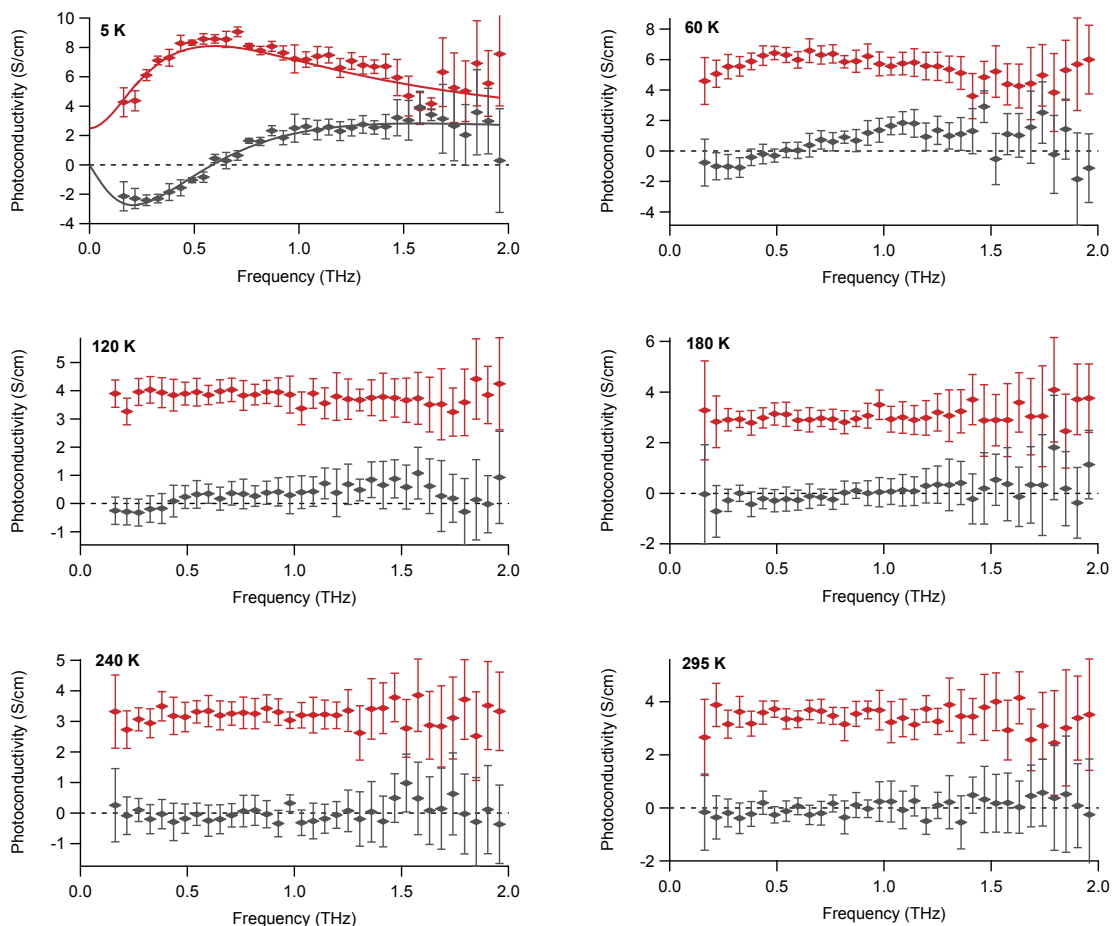


Figure S9. Frequency-dependent photoconductivity spectra for a FASnI_3 film with 10% added SnF_2 at temperatures from 5 – 295 K measured following photoexcitation at 800 nm. The spectra are averages of spectra recorded at 26 ps and 679 ps after excitation. For all of the spectra, the red traces are the real parts of the photoconductivity, and the gray traces are the imaginary parts. The solid lines on the graph showing data taken at 5 K indicate fits to the model described above.

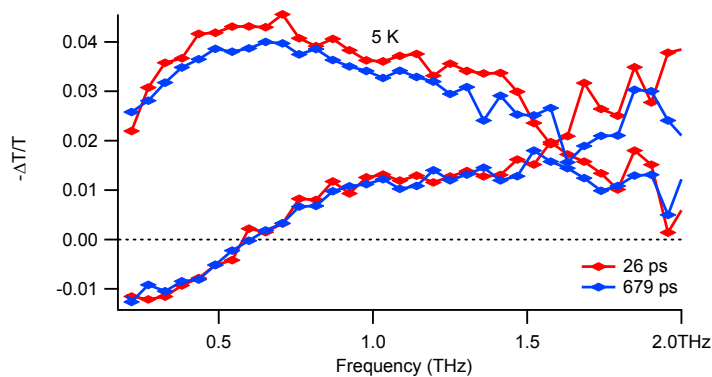


Figure S10. Time evolution of the photoconductivity spectrum measured at 5 K for a FASnI_3 film with 10% SnF_2 added during fabrication.

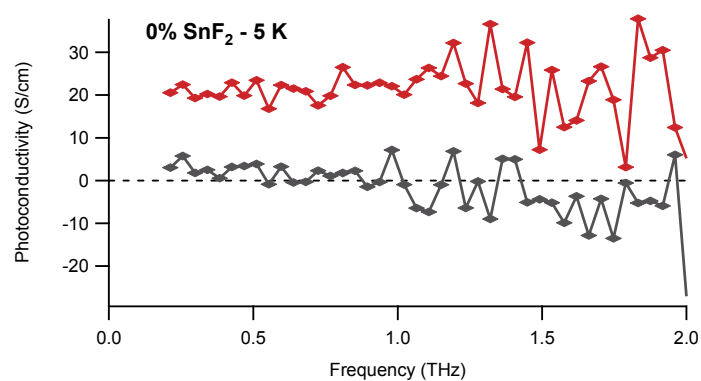


Figure S11. Photoconductivity spectrum for a FASnI₃ film with 0% SnF₂ added during fabrication measured at 5 K and photoexcited at 800 nm. The red trace is the real part of the photoconductivity, and the gray trace is the imaginary part.

8. References

- [1] J. S. Blakemore, *J. Appl. Phys.* **1982**, *53*, R123.
- [2] P. Umari, E. Mosconi, F. De Angelis, *Sci. Rep.* **2014**, *4*, 4467.
- [3] H. K. Nienhuys, V. Sundström, *Phys. Rev. B* **2005**, *71*, 235110.
- [4] R. Ulbricht, E. Hendry, J. Shan, T. F. Heinz, M. Bonn, *Rev Mod Phys* **2011**, *83*, 543.
- [5] R. A. Kaindl, D. Hagele, M. A. Carnahan, D. S. Chemla, *Phys. Rev. B* **2009**, *79*, 045320.